Article

Cell Reports

Two Independent Mushroom Body Output Circuits Retrieve the Six Discrete Components of *Drosophila* Aversive Memory

Graphical Abstract

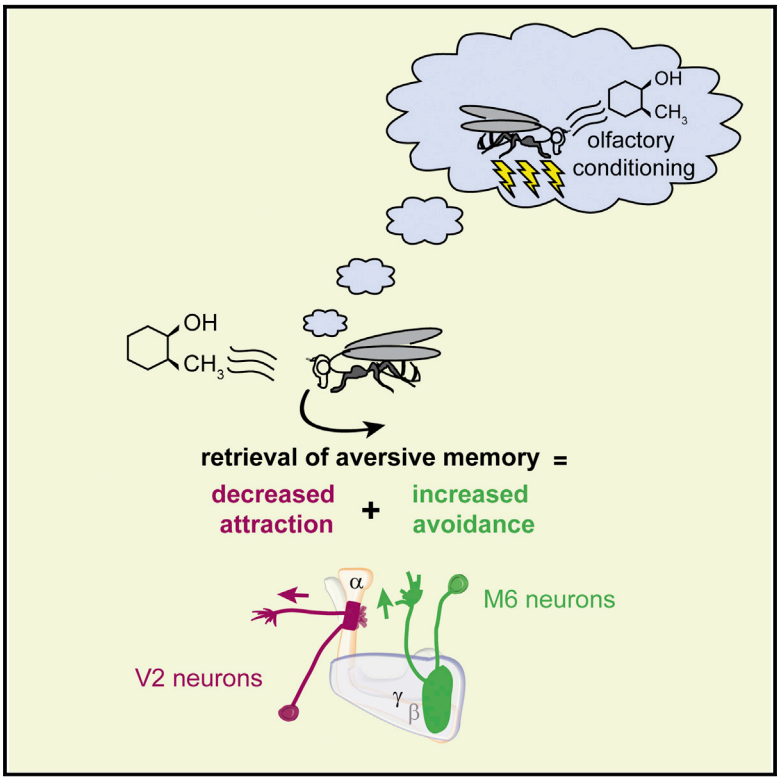

Authors

Emna Bouzaiane, Séverine Trannoy, ..., Pierre-Yves Plaçais, Thomas Preat

Correspondence

pierre-yves.placais@espci.fr (P.-Y.P.), thomas.preat@espci.fr (T.P.)

In Brief

Drosophila olfactory memory is composite, as is the structure of the mushroom body, the brain memory center. Through detailed circuit and behavioral analyses, Bouzaiane et al. describe six aversive memory phases localized within the mushroom body and characterize the output neurons that recall short-term memories.

Highlights

- Simultaneous memory phases are separately encoded within mushroom body neurons
- Glutamatergic M6 neurons retrieve memories from mushroom body γ neurons
- Cholinergic V2 neurons retrieve memories from mushroom body α/β neurons

Bouzaiane et al., 2015, Cell Reports *11*, 1280–1292
May 26, 2015
http://dx.doi.org/10.1016/j.celrep.2015.04.044

CellPress

OPEN ACCESS
CellPress

Cell Reports
Article

Two Independent Mushroom Body Output Circuits Retrieve the Six Discrete Components of *Drosophila* Aversive Memory

Emna Bouzaiane,[1] Séverine Trannoy,[1,3] Lisa Scheunemann,[1] Pierre-Yves Plaçais,[1,2,*] and Thomas Preat[1,2,*]
[1]Genes and Dynamics of Memory Systems, Brain Plasticity Unit, CNRS, ESPCI-ParisTech, PSL Research University, 10 rue Vauquelin, 75005 Paris, France
[2]Co-senior author
[3]Present address: Department of Neurobiology, Harvard Medical School, 220 Longwood Avenue, Boston, MA 02115, USA
*Correspondence: pierre-yves.placais@espci.fr (P.-Y.P.), thomas.preat@espci.fr (T.P.)
http://dx.doi.org/10.1016/j.celrep.2015.04.044

SUMMARY

Understanding how the various memory components are encoded and how they interact to guide behavior requires knowledge of the underlying neural circuits. Currently, aversive olfactory memory in *Drosophila* is behaviorally subdivided into four discrete phases. Among these, short- and long-term memories rely, respectively, on the γ and α/β Kenyon cells (KCs), two distinct subsets of the ~2,000 neurons in the mushroom body (MB). Whereas V2 efferent neurons retrieve memory from α/β KCs, the neurons that retrieve short-term memory are unknown. We identified a specific pair of MB efferent neurons, named M6, that retrieve memory from γ KCs. Moreover, our network analysis revealed that six discrete memory phases actually exist, three of which have been conflated in the past. At each time point, two distinct memory components separately recruit either V2 or M6 output pathways. Memory retrieval thus features a dramatic convergence from KCs to MB efferent neurons.

INTRODUCTION

Memory is not a singular entity but is based on distinct memory systems (Schacter and Tulving, 1994). Accordingly, memory is divided at the behavioral level into several discrete components referred to as memory phases. In a natural context where the brain integrates and retains memory of many experiences from diverse sensory modalities, these different forms of memory interact to guide proper behavior. How the different forms of memory interact within the brain is thus a central question in neurobiology and neuropsychology. A correlate of this question at the neural network level is whether a single memory-relevant circuit is capable of encoding different forms of memory.

Drosophila, which offer invaluable tools for neural network analysis, are capable of forming many different kinds of memory (Quinn and Dudai, 1976; Tempel et al., 1983; Tully et al., 1994; McBride et al., 1999; Liu et al., 2006; Colomb et al., 2009; Kaun et al., 2011). The associative aversive olfactory memory that results from a classical conditioning paradigm (in which an odorant is paired with the delivery of electric shocks) is the most thoroughly studied of these memory types. It features a complex pattern of memory phases (Tully et al., 1994; Isabel et al., 2004; Plaçais et al., 2012). Following a single cycle of conditioning, flies will retain memory of the odor-shock association for several hours. Cold anesthesia treatments have revealed that this memory is composite and made of an anesthesia-sensitive memory (ASM) component and an anesthesia-resistant memory (ARM) component (Quinn and Dudai, 1976). ASM and ARM are typically measured 3 hr after training, with a cold shock performed 2 hr after training (Lee et al., 2011; Plaçais et al., 2012; Scheunemann et al., 2012). By genetic analyses, ASM has been further divided into two temporal components: immediate short-term memory (STM), and middle-term memory (MTM) that occurs after approximately 1 hr (Quinn et al., 1979; Heisenberg, 2003; Lee et al., 2011).

Twenty-four hours after single-cycle training flies perform poorly in a memory test. Yet, flies are capable of forming long-lasting, consolidated memories after specific protocols. Following a spaced training protocol (composed of at least five cycles of conditioning spaced by rest intervals), flies form protein-synthesis long-term memory (LTM) that persists for several days (Tully et al., 1994), and which involves the activity of the CREB transcription factor (Yin et al., 1994). Using the same number of cycles without rest intervals (i.e., a massed training protocol) does not induce LTM formation but does promote instead a protein synthesis-independent consolidated ARM that decays within 48 hr (Plaçais et al., 2012; Tully et al., 1994). Several studies have identified genetic mutations that specifically affect memory 24 hr after spaced but not massed training (Comas et al., 2004; Didelot et al., 2006; Dubnau et al., 2003). Because they are both resistant to cold anesthesia, the consolidated ARM (as opposed to LTM) and the 3-hr ARM (as opposed to ASM) are widely confounded in the literature (see, e.g., Stough et al., 2006; Lee et al., 2011; Scheunemann et al., 2012). One study has also reported the existence of ARM immediately after training (Knapek et al., 2011), although this memory has not been further characterized.

The mushroom bodies (MBs) are the central integrative brain region for associative memory (de Belle and Heisenberg, 1994; Gerber et al., 2004; Krashes et al., 2007). MBs represent a paired structure of ~2,000 neurons per brain hemisphere, known as the Kenyon cells (KCs) (Aso et al., 2009). KCs receive dendritic input from the antennal lobes via projection neurons in the calyx area at the posterior part of the brain and send their axons anteriorly through a parallel bundle of fibers known as the peduncle. Based on their axonal morphology, KCs are classed into three different subtypes: axons from α/β and α′/β′ KCs branch at the anterior extremity of the peduncle to form the vertical (α and α′) and medial (β and β′) lobes, whereas axons from γ neurons form a single medial γ lobe (Crittenden et al., 1998). Beyond their anatomical distinctions, these subsets of KCs mediate memories of different persistence. STM is thought to be encoded in γ KCs (Blum et al., 2009; Qin et al., 2012) and LTM in α/β KCs (Blum et al., 2009; Pascual and Préat, 2001). A calcium LTM trace has been described in α lobes (Yu et al., 2006), but the STM trace in γ KCs remains unknown. Consistent with their role in memory encoding, signaling from KCs is crucial for memory retrieval. The use of the *Shibire*^{ts} (*Shi*^{ts}) transgenic thermosensitive dominant-negative allele of the dynamin-encoding gene *shibire*, expressed under the control of the UAS/GAL4 binary system, allows blocking of well-defined neuronal subsets with acute temporal resolution through temperature shifts (Kitamoto, 2001). This approach has been used in multiple studies to assess the role of the various subsets of KCs in memory retrieval at different time points after training. Indeed, previous reports have shown that immediate memory requires transmission from the α/β (McGuire et al., 2001), α′/β′ (Wang et al., 2008), and γ (Cervantes-Sandoval et al., 2013) KCs. Both α/β and γ KCs are also involved in memory retrieval at 2–3 hr (Isabel et al., 2004; Xie et al., 2013), when both ARM and MTM are present. Finally, the retrieval of LTM relies on α/β KC output (Isabel et al., 2004; Huang et al., 2013). Hence, several studies have attempted to delineate the KC subsets involved in aversive memory retrieval, but we still miss a clear picture of how these can be integrated with a "memory phase-aware" approach. Consequently, the study of the cellular mechanisms underlying the various memory phases and their interactions has been restricted. To reverse this trend, we challenged the correspondence between the behaviorally defined memory phases and the memory-relevant neuronal circuits at the network level.

Downstream of KCs, we previously described the functional role of neurons from the V2 cluster (which project from the MB vertical lobes) in memory retrieval, regardless of the test time or the conditioning protocol used (Séjourné et al., 2011). How STM, which is encoded in γ KCs, is retrieved thus remains an open question. Using behavioral analyses and live brain imaging, we characterized the role of a glutamatergic efferent circuit projecting from the tip of MB γ lobes in STM retrieval.

Our results have profound implications for the description of aversive memory phases. We have found that, like ASM, ARM is not a singular memory form but can be divided into three successive components that are spatially segregated. Overall, our study establishes that the composite nature of memory, as defined at the behavioral level, is mirrored at the network level by the existence of complementary circuits for memory retrieval. As a consequence, different memory phases that are behaviorally expressed at the same time do not share the same neuronal circuits.

RESULTS

An Immediate ARM Component Is Separately Encoded from Labile STM

It is generally believed that memory measured immediately after aversive training is made of anesthesia-sensitive STM, and that ARM is a consolidated memory phase formed approximately 1 hr later, which can last for 1–2 days after massed training (Lee et al., 2011; Scheunemann et al., 2012; Stough et al., 2006). However, one study recently reported that immediate memory contains an anesthesia-resistant component (Knapek et al., 2011). Therefore, we sought to localize this ARM component. We trained wild-type flies with single-cycle training and tested memory 5–7 min after training, with or without a 2-min cold anesthesia performed 2 min after training. Although the memory score was diminished by the cold treatment (which erased the anesthesia-sensitive part of the memory), a significant level of memory performance did persist (Figure 1A). This confirms that the major part of immediate memory corresponds to labile STM, although some ARM is present immediately after training.

In order to localize these memory components, we performed the same experiment at elevated temperature (33°C) with flies expressing Shi^{ts} in various KC subsets. To manipulate α/β KCs, we employed the widely used c739 GAL4 driver (McGuire et al., 2001; Isabel et al., 2004; Krashes et al., 2007; Aso et al., 2009; Trannoy et al., 2011) and the 44E04 line from the FlyLight GAL4 collection (Jenett et al., 2012) (Figure S1A; see also the FlyLight project website: http://flweb.janelia.org/cgi-bin/flew.cgi). Blocking α/β KCs impaired immediate memory performance (Figures 1B and 1C). When cold anesthesia was performed prior to the memory test, memory impairment was still observed. Previous controls for flies expressing Shi^{ts} with the c739 driver (McGuire et al., 2001) revealed normal immediate memory at the permissive temperature (25°C). We also verified that this was the case with the 44E04 driver (Figure S1C). Furthermore, blocking cell types labeled by these drivers did not alter naive olfactory acuity for the two odorants used in behavior experiments (Figure S1F; see Krashes and Waddell, 2008 for c739). These results indicate that the immediate ARM requires output from α/β neurons. We name this latter form of memory ST-ARM, for "short-term ARM." We then performed a similar set of experiments on γ KCs, using the 12E03 line from the FlyLight collection (Jenett et al., 2012) (Figure S1B; see also the FlyLight project website: http://flweb.janelia.org/cgi-bin/flew.cgi) and the NP21 GAL4 driver (Tanaka et al., 2008; Trannoy et al., 2011). Blocking γ KCs impaired immediate memory performance, but not after cold anesthesia (Figures 1D and 1E). Memory was normal at permissive temperature (Figures S1D and S1E), and olfactory acuity was not altered by neuronal blocking (Figures S1G and S1H). Therefore, these results indicate that the labile part of immediate memory (i.e., STM) requires output from the γ neurons.

Blocking α′/β′ KCs using the published GAL4 drivers 4-59 (Kaun et al., 2011) or G0050 (Wang et al., 2008) impaired ST-ARM performance 5 min after training (Figures S1L and S1M). However, 30 min after training, a time point that allows conditioning

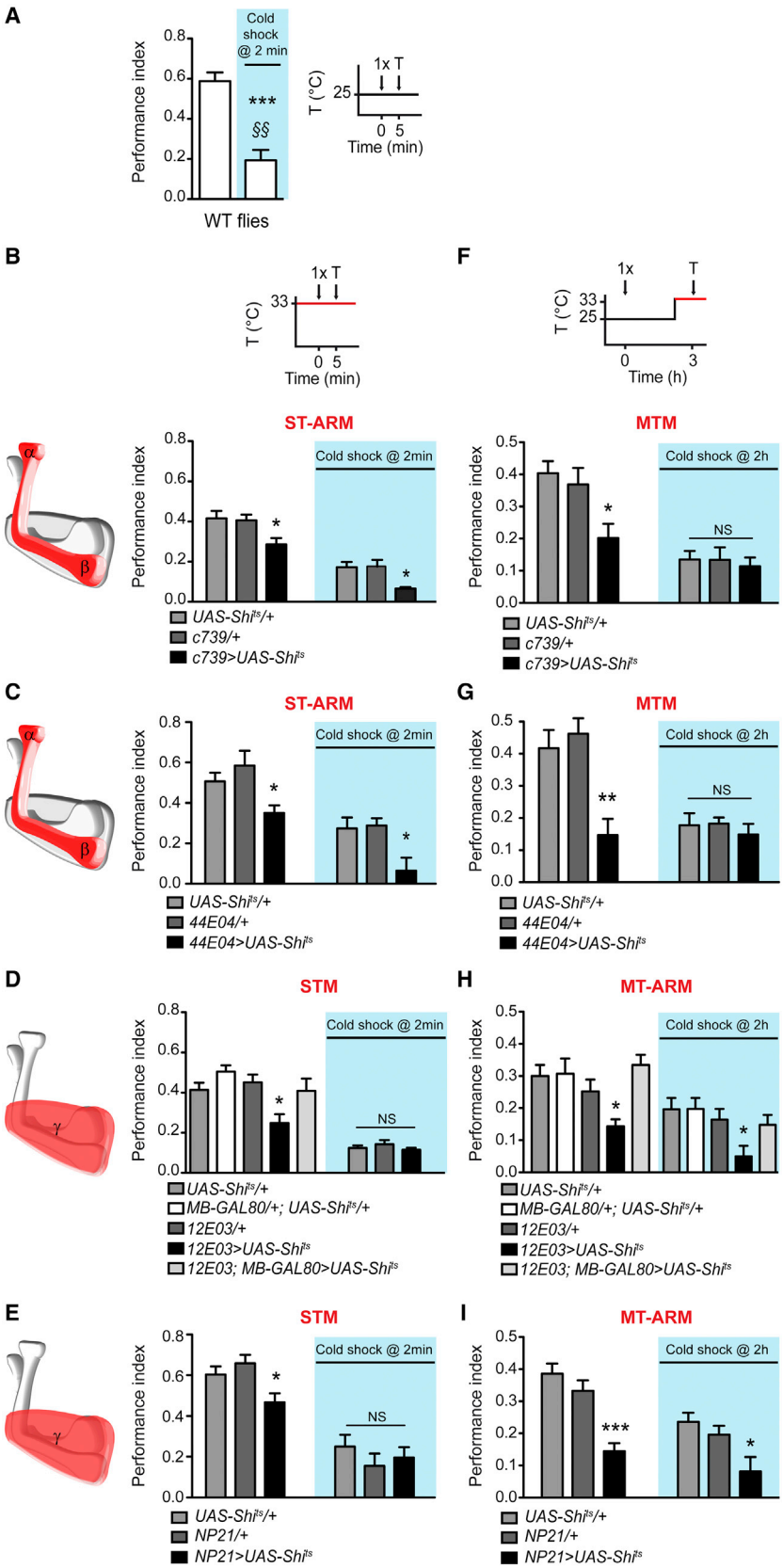

Figure 1. Alternated Localization of Short- and Middle-Term Memories

The temperature profile and time course of the experiment is provided next to the bar plot of performance indices (1×, single-cycle training; T, memory test). In experiments involving neuronal blocking with *Shi*^{ts}, the neurons that are blocked during periods at restrictive temperature are highlighted in red on the sketches. The memory phase that is affected by neuronal block is displayed in red above the graph. All cold shocks lasted 2 min. The time when cold shock occurred is stated on the graph.

(A) The immediate memory of wild-type (WT) *CS* flies was significantly decreased by a cold shock performed between training and the memory test (t test, $t_{(14)} = 5.88$, ***$p < 0.0001$, $n = 8$). This impairment was only partial (one-sample t test compared to 0, $t_{(7)} = 3.79$, §§$p = 0.0068$), revealing anesthesia-resistant memory.

(B–E) Flies were trained and tested for immediate memory at restrictive temperature. Flies expressing *Shi*^{ts} in α/β KCs with the c739 driver or with the 44E04 driver displayed impaired immediate memory (B: $F_{(2,23)} = 6.60$, $p = 0.006$, $n = 11$; C: $F_{(2,18)} = 5.41$, $p = 0.016$, $n = 6–7$), which was also measurable after cold-shock treatment (B: $F_{(2,32)} = 4.81$, $p = 0.012$, $n = 8$; C: $F_{(2,20)} = 5.28$, $p = 0.016$, $n = 6–8$). Flies expressing *Shi*^{ts} in γ KCs with the 12E03 driver or the NP21 driver displayed impaired immediate memory. Due to the wide additional expression pattern of the 12E03 driver (Figure S1B), we performed a parallel rescue experiment using the *MB-GAL80* transgene, which inhibits GAL4 action specifically in the MB (D: $F_{(4,49)} = 4.78$, $p = 0.0027$, $n = 10$; E: $F_{(2,31)} = 5.60$, $p = 0.0088$, $n = 10–11$). No defect was observed after cold-shock treatment. (D: $F_{(2,29)} = 0.88$, $p = 0.43$, $n = 10$; E: $F_{(2,19)} = 0.65$ $p = 0.53$, $n = 6–8$).

(F–I) Flies were trained with a single cycle and tested 3 hr later at the restrictive temperature. Flies expressing *Shi*^{ts} in α/β KCs displayed an impaired 3-hr memory (F: $F_{(2,17)} = 5.79$, $p = 0.014$, $n = 6$; G: $F_{(2,29)} = 10.74$, $p = 0.0004$, $n = 10$); however, no defect was observed when a cold shock was performed 2 hr after training (F: $F_{(2,44)} = 0.15$, $p = 0.87$, $n = 15$; G: $F_{(2,28)} = 0.35$, $p = 0.70$, $n = 9–10$). Flies expressing *Shi*^{ts} in γ KCs with the 12E03 driver displayed impaired 3-hr memory, which could be rescued by combination with *MB-GAL80* ($F_{(4,79)} = 4.55$, $p = 0.0024$, $n = 16$). The defect was still measurable after cold shock ($F_{(4,79)} = 3.31$, $p = 0.015$, $n = 16$), showing that the 3-hr memory retrieved from γ KCs corresponds to MT-ARM. Similar results were obtained with the NP21 driver (no cold shock: $F_{(2,32)} = 17.59$, $p < 0.0001$, $n = 11$; cold shock: $F_{(2,44)} = 5.36$, $p = 0.0085$, $n = 15$).

Data are mean ± SEM. *$p < 0.05$; **$p < 0.01$; ***$p < 0.0001$; NS, not significant. See Experimental Procedures for further details on statistical analyses. STM, short-term memory; ST-ARM, short-term anesthesia-resistant memory; MTM, middle-term memory; MT-ARM, middle-term anesthesia-resistant memory. See also Figure S1.

at permissive temperature, there was no defect in a similar experiment (Figures S1N and S1O), while blocking α/β KCs at that time point still impaired ST-ARM (Figure S1P). This suggests that output from α′/β′ KCs is required during training for ST-ARM formation but dispensable for ST-ARM retrieval. This confirms the role of α′/β′ KCs during training (Krashes et al., 2007). Using a similar thermal blocking protocol and the c305 GAL4 driver, it was reported that α′/β′ KCs are required for the retrieval of 30-min memory (Cervantes-Sandoval et al., 2013). While we indeed observed a memory defect using this driver, we also observed that this defect persisted when the whole protocol was performed at the 25°C control temperature (Figure S1Q). It should be noted that this defect at permissive temperature was not detected in the aforementioned study (Cervantes-Sandoval et al., 2013), because this requires the direct statistical comparison of the *c305-GAL4>UAS-Shi^{ts}* genotype with its *c305-GAL4*/+ and *UAS-Shi^{ts}*/+ controls, as it is classically done. On the contrary, Cervantes-Sandoval et al. (2013) did not compare the score of *c305-GAL4>UAS-Shi^{ts}* flies with the scores of the genotypic controls but instead compared the scores of *c305-GAL4>UAS-Shi^{ts}* flies at restrictive and permissive temperature. Thus, the data obtained with the c305 driver are not usable to conclude that output from α′/β′ KCs is required during 30-min memory retrieval. To summarize, our results show that STM and ST-ARM are separately encoded in MB neurons. STM retrieval involves γ KCs and ST-ARM retrieval involves α/β KCs.

Labile MTM Is Encoded Separately from ARM

Is ST-ARM an early manifestation of the singular ARM, or is it a new memory phase? To investigate this question, we aimed to localize the KCs underlying ARM retrieval at later time points. It is well established that 3-hr memory after single-cycle training is a composite of labile MTM and ARM. If ARM is a singular phase, we would expect 3-hr ARM ("middle-term ARM" or MT-ARM) to be localized in the same KCs as ST-ARM. Blocking α/β KCs during memory retrieval did impair memory, but memory impairment was absent when a 2-min cold shock was performed 1 hr prior to the test to remove the MTM fraction (Figures 1F and 1G). This reveals that α/β KCs mediate labile MTM rather than MT-ARM. Conversely, blocking γ KCs decreased 3-hr memory, and the memory drop was still present after cold shock, indicating that MT-ARM is affected (Figures 1H and 1I). We verified the absence of any defect whether the memory test was performed at the permissive temperature (Figures S1I–S1K). Blocking α′/β′ KCs had no effect on 3-hr memory retrieval (Figures S1R and S1S), as previously reported (Krashes et al., 2007). Thus, as for immediate memory, MT-ARM and MTM are spatially separated within KCs. At this time point and contrary to what was observed immediately after training, γ KCs mediate the retrieval of the ARM component and α/β KCs mediate the retrieval of labile MTM. From a previous series of continuous blocking experiments performed in our laboratory, where cold shock was performed 1 hr after training and memory was measured 1 hr later (Isabel et al., 2004), it had been concluded that 2-hr ARM was located in the α/β KCs and labile memory in γ KCs, a pattern similar to what we observed here in the short-term range. We repeated these experiments and obtained results similar to the pattern of middle-term memory components, with 2-hr ARM located in γ KCs (Figures S1T and S1U). The results from these two series of data suggest that STM and ST-ARM had a longer persistence at the time of our earlier experiments, and that the time period around 1 hr following training, when the cold shock was performed in these experiments, is a critical time period for the transition from the short- to the middle-term patterns of memory phases. Indeed, if the transition occurs around 1 hr after training, it is conceivable that a small shift in the timing of this transition in the fly brain (e.g., 1 hr 15 min versus 45 min) would yield seemingly opposite results (see Experimental Procedures for a possible explanation of this time shift).

The important finding brought by the present detailed analysis is that, as is true for labile memory, ARM includes distinct successive components, which are separately encoded from the corresponding labile memory phases.

V2 Neurons Retrieve Memory Phases Encoded in α/β KCs

Our dissection of KC involvement in memory retrieval revealed that at a given time point each memory phase can be unequivocally assigned to a precise subset of KCs. Is this reflected in the downstream stage of MB output neurons? A unique ensemble of cholinergic MB efferent neurons, known as V2 neurons (Tanaka et al., 2008), has previously been described as required for aversive memory retrieval. The V2 cluster contains approximately ten neurons that are anatomically subdivided into V2α neurons, projecting from the α vertical lobe, and V2α′ neurons, projecting from the α′ vertical lobe (Séjourné et al., 2011). The 71D08 GAL4 driver targets the whole population of V2 neurons and the MZ160 GAL4 driver only targets the V2α neurons (Séjourné et al., 2011). Blocking neurotransmission from V2α neurons impairs immediate and 2-hr memory after single-cycle training (Séjourné et al., 2011). After showing that immediate memory is actually composite and ARM is not a singular memory phase, we inquired whether all forms of memory are indeed retrieved through this circuit. We confirmed that blocking either all V2 neurons or V2α neurons impairs immediate memory and observed that impairment still occurs when a cold shock is administered between training and the memory test (Figures 2A and 2B), indicating that V2α neurons are required for ST-ARM retrieval. This is in accordance with data provided in Figure 1, illustrating that ST-ARM rely on signaling from α/β KCs. Blocking all V2 neurons or V2α neurons caused a memory defect in 3-hr memory retrieval, which disappeared if a cold shock was performed prior to the memory test (Figures 2C and 2D). Thus, V2α neurons mediate MTM retrieval, but they are dispensable for MT-ARM retrieval. This is consistent with our finding that MTM retrieval involves only α/β KCs (Figure 1). Combined, our data show that V2 neurons do not comprehensively retrieve memory from KCs; instead, they consistently mediate the retrieval of memory phases encoded in α/β neurons. The two memory phases that were not affected by V2 blockade, STM and MT-ARM, rely on γ KCs. This prompted us to search for γ-lobe efferent neurons that could mediate these memories.

M6 Neurons Function as a Complementary Retrieval Pathway from γ KCs

To identify MB-output neurons involved in the retrieval of memories encoded in γ KCs, we selected GAL4 lines from the NP collection that target every type of γ KC-connected extrinsic neuron described in Tanaka et al. (2008). Using *Shi^{ts}*, we tested

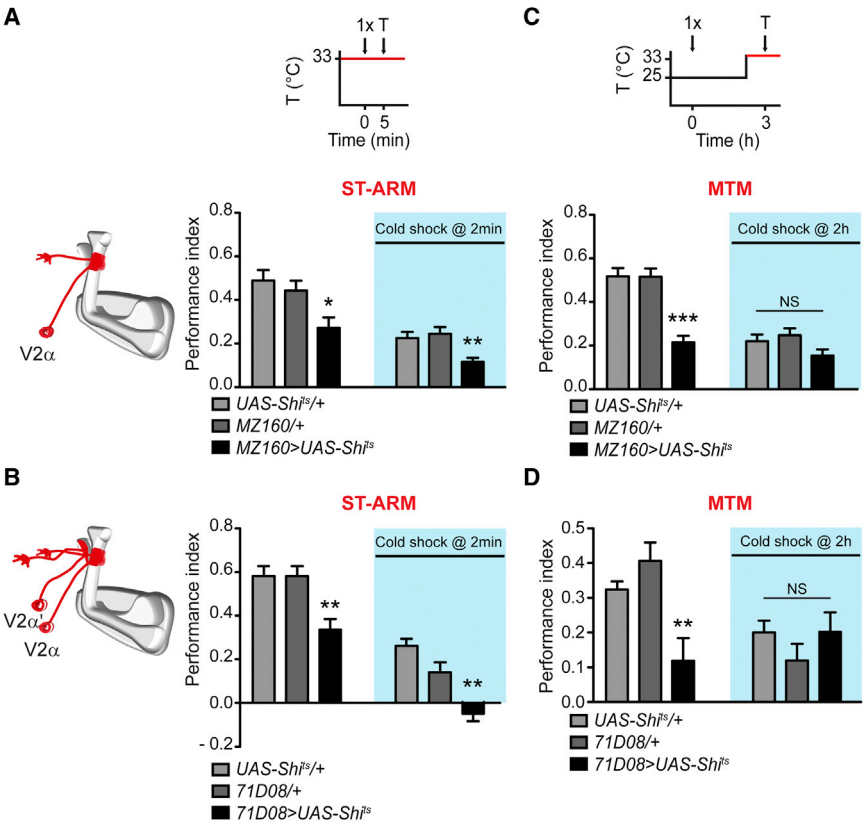

Figure 2. V2 Neurons Do Not Retrieve All Forms of Aversive Memory

(A and B) Flies were trained and tested for immediate memory at restrictive temperature. Flies expressing *Shi*^{ts} in V2α neurons with the MZ160 driver, or in all V2 neurons with the 71D08 driver, displayed impaired immediate memory (A: $F_{(2,26)} = 5.91$, $p = 0.0082$, $n = 9$; B: $F_{(2,30)} = 9.48$, $p = 0.0007$, $n = 10–11$), which was also measurable after a cold-shock treatment (A: $F_{(2,29)} = 6.97$, $p = 0.0036$, $n = 10$; B: $F_{(2,22)} = 11.76$, $p = 0.0004$, $n = 6–10$).

(C and D) Flies were trained with a single cycle and tested 3 hr later at the restrictive temperature. Flies expressing *Shi*^{ts} in V2α neurons with the MZ160 driver, or in all V2 neurons with the 71D08 driver, displayed impaired 3-hr memory (C: $F_{(2,47)} = 23.56$, $p < 0.0001$, $n = 16$; D: $F_{(2,23)} = 8.58$, $p = 0.0019$, $n = 8$) but did not display impaired memory after a cold-shock treatment (C: $F_{(2,65)} = 2.62$, $p = 0.081$, $n = 21$; D: $F_{(2,29)} = 1.00$, $p = 0.38$, $n = 10$).

Data are mean ± SEM. *$p < 0.05$; **$p < 0.01$; ***$p < 0.0001$; NS, not significant. See Experimental Procedures for further details on statistical analyses. See also Figure S2.

the effect of blocking neurons labeled by each line during the retrieval of 3-hr memory after a single training (Figure S2A). From this preliminary screen, we isolated the NP3212 line (Figure S2B), which is reported to label two types of MB-extrinsic neurons: the M4 neurons (two per hemisphere) and the M6 neurons (one per hemisphere) that contact the tip of medial lobes. Blocking the NP3212-positive neurons during the retrieval of 3-hr memory caused a memory defect, which was still measurable after a cold shock (Figure S2C). No defect was observed when the experiment was performed at the permissive temperature (Figure S2D). Moreover, blocking NP3212 neurons during and after training (but not during the memory test) did not affect memory (Figure S2E). Blocking NP3212 neurons did not alter the olfactory acuity (Figure S2F). These data suggest that the M4/M6 cluster plays a major role in MT-ARM retrieval. Careful examination of the NP3212 expression pattern revealed weak and sparse expression in α/β KCs that could be prevented by combination with the MB-GAL80 transgene (data not shown). We could still observe the memory retrieval defect in combination with MB-GAL80 (Figure S2G). This provides further evidence that the memory retrieval phenotypes could be due to the M4/M6 neurons. Interestingly, M4 and M6 neurons have recently been anatomically characterized as glutamatergic MB-efferent neurons (Aso et al., 2014a). Dendrites from M4 neurons arborize on the tip of β′ lobes, and dendrites from M6 neurons cover the tip of γ lobes and also connect the most ventral part of β′ lobes. Both cell types project in the superior medial protocerebrum (SMP) (Tanaka et al., 2008; Aso et al., 2014a) (Figure S2B).

We identified two additional GAL4 drivers from the FlyLight collection (Jenett et al., 2012) that label the M4/M6 cluster, the 14C08 and 27G01 lines (Figures 3A and 3B; see also the FlyLight project website for movies: http://flweb.janelia.org/cgi-bin/flew.cgi). At this resolution, we did not observe any additional overlapping expression pattern between the two drivers. To further characterize the retrieval of memories encoded in γ KCs, we expressed *Shi*^{ts} with these two drivers and tested immediate memory at the restrictive temperature. Both lines exhibited a defect (Figures 3C and 3D), which did not occur at the permissive temperature (Figures S3A and S3B). Blocking 14C08- or 27G01-positive neurons did not alter naive odor avoidance (Figures S3C and S3D). In addition, no defect was observed in immediate memory when a cold shock was performed between training and the test (Figures 3C and 3D). These results point to a role of M4/M6 neurons in STM. When 3-hr memory was tested at restrictive temperature, both lines also yielded defects, which was also observed when a cold shock was performed prior to the memory test (Figures 3E and 3F, and Figures S3E and S3F for permissive temperature controls). By contrast, blocking during and after training (but not during the memory test) had no effect on 3-hr memory (Figures S3G and S3H). This indicates that M4/M6 neurons are specifically involved in the retrieval of MT-ARM. These results are identical to those we obtained for the NP3212 line (Figure S2). Altogether, the consistent data obtained from these three distinct drivers strongly support a role for the M4/M6 cluster in the retrieval of STM and MT-ARM, the two memory phases that involve γ KCs.

In order to dissociate the role of the M4 and M6 neurons, we selected the VT46095 and 12C11 GAL4 lines from the Vienna Tile collection and the FlyLight collection, respectively. The VT46095 line labels M6 but not M4 neurons, whereas the

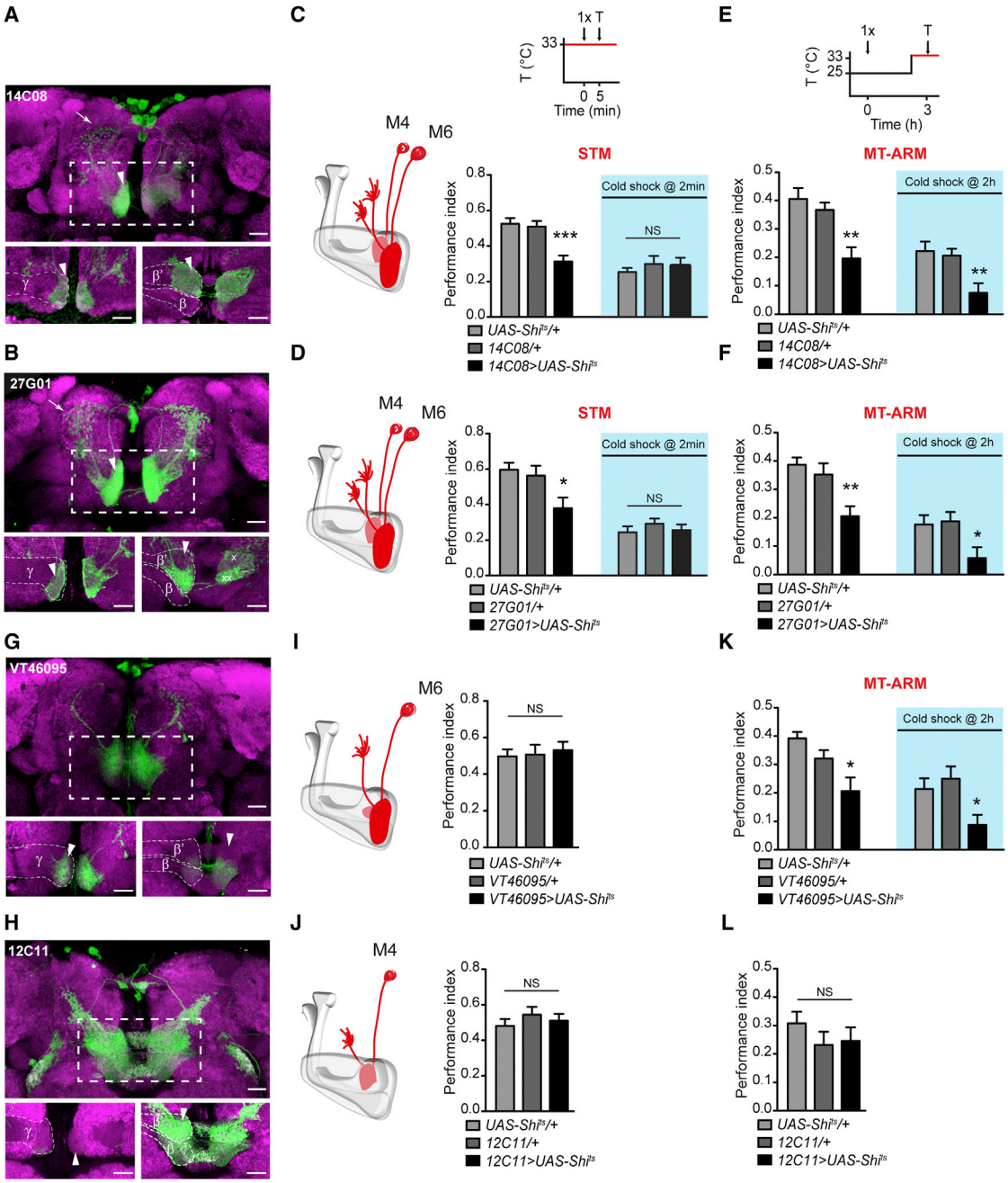

Figure 3. M6 Neurons Retrieve Memory from γ KCs

(A and B) Projection of confocal stacks showing the expression pattern of the 14C08 and 27G01 drivers in the region of the MB lobes (green, mCD8::GFP; magenta, nc82 counterstaining). Both lines displayed labeled terminals in the SMP region (arrows) that were characteristic of M4 and M6 neurons, as well as arborizations on the tip of medial lobes (arrowheads). Below the projection images, single slices show arborizations from M6 and M4 neurons on γ and β′ lobes, respectively (arrowheads). Note that in 27G01, the innervation on β′ lobes by M4 neurons is faint ("x"), which underscores a more intense innervation on the ventral part of the lobe belonging to M6 neurons ("xx"). Scale bars, 20 μm.

(C and D) Flies were trained and tested for immediate memory at high temperature. Flies expressing Shi^{ts} in M4 and M6 neurons with the 14C08 driver displayed impaired immediate memory ($F_{(2,38)} = 13.46$, $p < 0.0001$, $n = 13$), which could not be measured after cold-shock treatment ($F_{(2,23)} = 0.36$, $p = 0.70$, $n = 8$). Similar results were obtained with the 27G01 driver (no cold shock: $F_{(2,23)} = 4.84$, $p = 0.019$, $n = 8$; cold shock: $F_{(2,29)} = 0.61$, $p = 0.55$, $n = 10$).

(E and F) Flies were trained with a single cycle and tested 3 hr later at the restrictive temperature. Flies expressing Shi^{ts} in M4 and M6 neurons with the 14C08 driver displayed impaired 3-hr memory ($F_{(2,32)} = 10.03$, $p = 0.0005$, $n = 11$), which was still measurable after cold shock ($F_{(2,50)} = 6.71$, $p = 0.0027$, $n = 17$). Similar results were obtained with the 27G01 driver (no cold shock: $F_{(2,26)} = 8.17$, $p = 0.0020$, $n = 9$; cold shock: $F_{(2,26)} = 4.33$, $p = 0.025$, $n = 9$).

(legend continued on next page)

12C11 line conversely labels M4 but not M6 neurons (Figures 3G and 3H). The VT46095 line displayed partial labeling of the most ventral part of the β′ lobe, which in the absence of M4 neuron expression could be attributed to the M6 neurons (Figure 3G), confirming our previous observation with the 27G01 line and in accordance with another report (Aso et al., 2014a). The VT46095 and 12C11 lines both label an additional type of β-lobe connected neurons known as MBON-β2β′2a (Aso et al., 2014a). These two lines thus enabled us to address the role of M4 and M6 neurons in memory retrieval separately. Immediately after training, we could not observe any memory impairment with either line (Figures 3I and 3J), but when the two drivers were combined, immediate memory was indeed impaired (Figure S3I) suggesting that blocking both M4 and M6 neurons is required to prevent STM retrieval. Nonetheless, blocking M6 neurons alone with VT46095 impaired 3-hr memory retrieval both with and without cold shock (Figure 3K and Figure S3J for permissive temperature control), and it did not alter naive odor avoidance (Figure S3K). By contrast, no defect was observed when M4 neurons were blocked using the 12C11 line (Figure 3L). This indicates that only the M6 neurons, which project from the γ lobes, mediate MT-ARM retrieval. This is consistent with the retrieval of MT-ARM through γ KCs (Figure 1D).

M6 Neuron Activity Is Enhanced 3 hr after Training in Response to the Conditioned Odorant

In a previous study, we observed that V2 neurons exhibit a brief yet strong increase in activity upon olfactory perception, as reported by calcium imaging using GCaMP3 (Séjourné et al., 2011). We also showed that, 3 hr after single-cycle training, the response to the conditional stimulus CS^+ (i.e., the trained odorant) was diminished as compared to the unconditional stimulus CS^- (i.e., the odorant that was not associated with electric shocks). Here, we similarly chose to study the training-induced changes in the physiology of M6 neurons by live imaging experiments. We employed the VT46095 driver for our imaging experiments, to avoid any confusion with M4 neurons that innervate similar regions as the M6 neurons. We trained flies with a single-cycle conditioning and recorded their response to a 5-s delivery of CS^+ and CS^-. The measurements were performed between 2.5 and 3.5 hr after training, a time point in which M6 neurons support the MT-ARM retrieval (Figure 3). In the presynaptic terminals of M6 neurons in the dorsal part of the SMP (Figure 4A), we observed moderate odor-induced variations that were variable among different individuals. On average, the response to the CS^+ was higher than to the CS^- (Figure 4B). Noticeably, the difference between the CS^+ and CS^- time traces far exceeded the duration of the olfactory stimulation (gray window in Figure 4B). As a control, we trained flies with an unpaired protocol that does not yield any memory, by temporally separating electric shocks from odor delivery. No difference was observed in these flies between their responses to the two odors (Figure 4C). Finally, we observed that the response to the CS^+ was also enhanced in flies that were administered a cold shock 2 hr after training (Figure 4D). Comparing the data obtained with the three protocols clearly revealed an enhanced response to the CS^+ odor induced by the associative training, which outlasted the period of olfactory stimulation by more than 10 s (Figure 4E). Overall, our data indicate that MT-ARM retrieval relies on a moderate but sustained increase in M6 neuron activity. Olfactory responses of γ KCs in the γ lobes were also recorded, and no training-induced change in the responses to CS^+ and CS^- could be detected (Figure S4). This suggests that plasticity occurs at the synapses between γ KCs and M6 neurons that results in the increased CS^+ response we evidenced in M6 neurons.

Long-Term ARM Involves the α′/β′ KC-M6 Neurons Circuit

ARM has been historically described as the fraction of 3-hr memory that is resistant to cold anesthesia, but also as the protein synthesis-independent form of consolidated memory that forms after massed training and lasts 24–48 hr (Tully et al., 1994). We verified that the memory measured 24 hr after massed training in wild-type flies was resistant to cold anesthesia (Figure S5A). Since ST-ARM and MT-ARM could be distinguished, we wondered whether ARM measured 24 hr after massed training was yet a distinct form of ARM. Strikingly, the pattern of KCs required for memory retrieval 24 hr after massed training was again distinct from what we observed for immediate and 3-hr memory. Blocking α′/β′ KCs caused a memory impairment (see Figures 5A, S5B, and S5C for permissive temperature and olfactory acuity controls), whereas blocking α/β or γ KCs had no effect (Figures 5B and 5C). 24-hr ARM therefore involves α′/β′ neurons. We asked whether the difference between experiments performed 3 hr after single-cycle training and 24 hr after massed training was due to the time point at which memory was tested or to the difference in conditioning protocols. We observed that, 3 hr after massed training, blocking α/β KCs impaired the labile part of memory, blocking γ KCs impaired ARM, and blocking α′/β′ KCs had no effect (Figures S5D–S5F). These findings recapitulate the results obtained 3 hr after single-cycle training. Thus,

(G and H) Projection of confocal stacks showing the expression pattern of the VT46095 and 12C11 drivers in the region of the MB lobes (green: mCD8::GFP; magenta: nc82 counterstaining). VT46095 shows strong GFP expression on the tip of γ lobes but almost none on β′ lobes (arrowheads), except for the M6 neuron processes on the most ventral part of β′ lobes. 12C11 shows no GFP expression on the γ lobes but entirely covers the tip of β′ lobes (arrowheads). Both lines also label a pair of neurons innervating the tip of the β lobe. Scale bars, 20 μm.

(I) Flies were trained and tested for immediate memory at high temperature. Flies expressing Shi^{ts} solely in M6 neurons with the VT46095 driver did not display any memory defect ($F_{(2,42)} = 0.13$, $p = 0.87$, $n = 14–15$).

(J) Flies expressing Shi^{ts} solely in M4 neurons with the 12C11 driver did not display any memory defect ($F_{(2,23)} = 0.63$, $p = 0.54$, $n = 8$).

(K) Flies were trained with a single cycle and tested 3 hr later at the restrictive temperature. Flies expressing Shi^{ts} in M6 neurons with the VT46095 driver displayed impaired 3-hr memory ($F_{(2,35)} = 7.20$, $p = 0.0025$, $n = 12$), which was still measurable after cold shock ($F_{(2,29)} = 4.8$, $p = 0.017$, $n = 10$).

(L) Conversely, flies expressing Shi^{ts} in M4 neurons with the 12C11 driver displayed normal 3-hr memory ($F_{(2,29)} = 0.81$, $p = 0.46$, $n = 10$).

Data are mean ± SEM. *$p < 0.05$; **$p < 0.01$; ***$p < 0.0001$; NS, not significant. See Experimental Procedures for further details on statistical analyses. See also Figure S3.

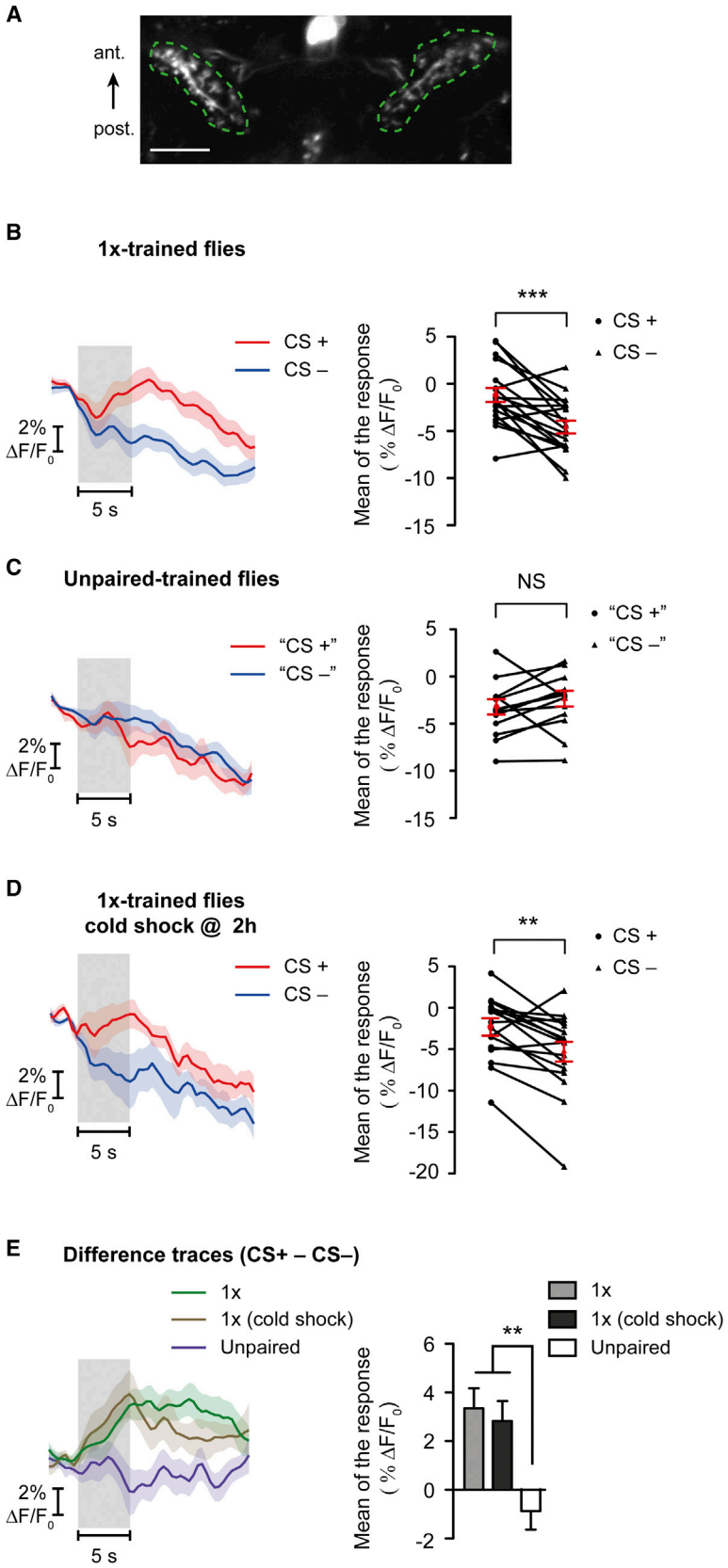

Figure 4. Response of M6 Neurons to the Trained Odorant Is Increased 3 hr after Training

(A) The calcium reporter GCaMP3 was expressed in M6 neurons with the VT46095 driver. Transverse sections of the brain were imaged, and fluorescence was monitored from dorsal terminals of M6 neurons (dashed regions of interest). Scale bar, 20 μm.

(B) Flies were trained with a single-cycle protocol and imaged 2.5–3.5 hr later. Average time traces of M6 neuron activity upon presentation of the two odors used during training are displayed (see Experimental Procedures for details on data analysis). The gray area indicates the 5-s-long period of odor delivery. After an initial drop, the CS^+ trace was consistently situated above the CS^- trace. This difference largely outlasted the time of odor perception. Accordingly, the mean response to the CS^+ was higher than to the CS^- (paired t test, $t_{(18)} = 4.48$, ***p = 0.0003, n = 19).

(C) In flies that were subjected to an unpaired training protocol (odors delivered separately from shocks; see Experimental Procedures for details), no difference was observed between the responses to the two odors (paired t test, $t_{(12)} = 1.14$, p = 0.28 [NS, not significant], n = 13. "CS^+", first odor delivered 2 min after electric shocks; "CS^-", second odor delivered).

(D) The increased response to CS^+ in trained flies was still present when a cold shock was performed 2 hr after training (paired t test, $t_{(16)} = 3.49$, **p = 0.003, n = 17).

(E) The difference traces allow direct comparison between the different protocols. Associative training resulted in a moderate but sustained enhancement of the CS^+ response relative to CS^-, which was absent in unpaired-trained flies (two-way repeated-measures ANOVA (Time, Protocol): $F^{Protocol}_{(2,1794)} = 6.88$, p = 0.0024). The mean [CS^+ to CS^-] responses calculated from these difference traces were also significantly different ($F_{(2,48)} = 6.86$, p = 0.0025, n = 13–19).

Data are mean ± SEM. See also Figure S4.

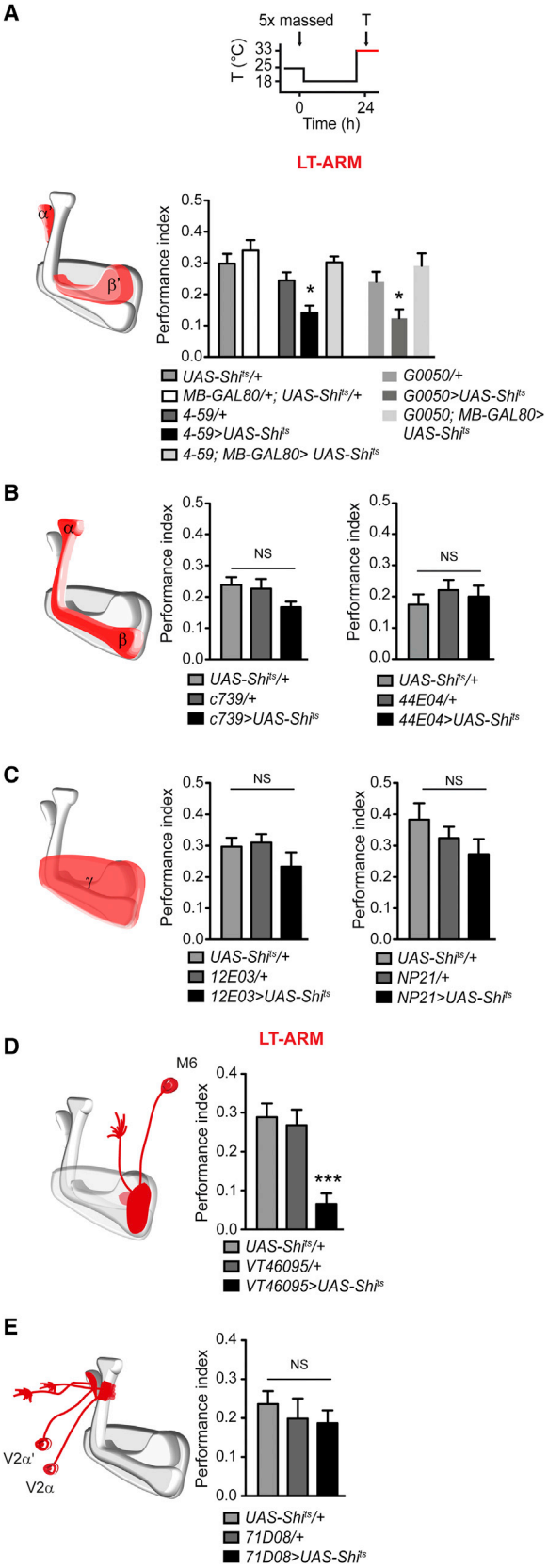

Figure 5. Retrieval Circuit of Consolidated Memory after Massed Training

(A–E) Flies were trained with a massed protocol and tested 24 hr later at the restrictive temperature. No cold shock was performed in these experiments because the memory measured 24 hr after massed training is essentially made of ARM (Figure S5A). Flies expressing Shi^{ts} in α'/β' KCs with the 4-59 or G0050 drivers displayed a memory defect 24 hr after massed training. The defect induced by either driver was rescued by combination with *MB-GAL80* ($A: F_{(7,80)} = 6.98$, $p < 0.0001$, $n \geq 9$). Flies expressing Shi^{ts} in α/β KCs with the c739 driver or the 44E04 driver displayed normal LT-ARM performance (B: c739: $F_{(2,35)} = 2.3$, $p = 0.12$, $n = 12$; 44E04: $F_{(2,32)} = 0.48$, $p = 0.62$, $n = 11$). Flies expressing Shi^{ts} in γ KCs with the 12E03 driver or the NP21 driver displayed normal LT-ARM performance (C: 12E03: $F_{(2,29)} = 1.42$, $p = 0.26$, $n = 9$; NP21: $F_{(2,37)} = 1.43$, $p = 0.25$, $n = 12$). Blocking M6 neurons with the VT46095 driver impaired LT-ARM retrieval (D: $F_{(2,29)} = 12.77$, $p = 0.0001$, $n = 10$). Flies expressing Shi^{ts} in all V2 neurons using the 71D08 driver displayed normal LT-ARM performance (E: $F_{(2,44)} = 0.41$, $p = 0.67$, $n = 15$). Data are mean ± SEM. $^*p < 0.05$; $^{***}p < 0.0001$; NS, not significant. See Experimental Procedures for further details on statistical analyses. LT-ARM, long-term anesthesia-resistant memory. See also Figure S5.

persistence, and not the training protocol, determines the spatial localization of ARM. Distinctly from ST-ARM and MT-ARM, the "long-term ARM" (LT-ARM) is retrieved from α'/β' KCs. Which MB output circuit mediates LT-ARM retrieval? Blocking M4/M6 neurons (Figures S5G–S5J) or M6 neurons only (Figure 5D; Figure S5K) during memory retrieval 24 hr after massed training almost fully abolished LT-ARM. Blocking M4 neurons alone had no effect (Figure S5L). By contrast, blocking V2 neurons using the 71D08 GAL4 driver did not affect LT-ARM retrieval (Figure 5E). Our data therefore indicate that LT-ARM is retrieved from α'/β' KCs solely by M6 neurons and not by V2 neurons, despite our former conclusions (Séjourné et al., 2011; see Figures S5O–S5R and Discussion). Conversely, M4/M6 neurons are dispensable for the retrieval of LTM 24 hr after spaced training (Figures S5M and S5N), contrary to V2 neurons (Séjourné et al., 2011; Aso et al., 2014b).

The Dunce Phosphodiesterase Supports All Forms of ARM

At the molecular level, several genes were shown to support ARM. In particular, the phosphodiesterase-encoding *dunce* (*dnc*) gene, one of the first memory genes identified in *Drosophila* (Dudai et al., 1976), underlies 3-hr ARM, that we here named MT-ARM (Scheunemann et al., 2012). We therefore asked whether Dnc is involved in ST-ARM, MT-ARM, and LT-ARM in their respective subpopulations of KCs. We expressed a previously characterized RNAi against *dnc* (Scheunemann et al., 2012) in the various subsets of KCs that we showed underlie the sequential ARM phases. Strikingly, knockdown of *dnc* in the α/β KCs impaired ST-ARM performance (Figure 6A). By contrast, MT-ARM was not impaired by the RNAi expression in γ KCs (Figure 6B), in accordance with the localization of *dnc* action outside KCs for 3-hr ARM (Scheunemann et al., 2012). Finally, RNAi expression in α'/β' KCs did impair LT-ARM performance (Figure 6C). Therefore, *dnc* supports all forms of ARM. ST-ARM and LT-ARM require *dnc* activity in the same neurons as those from which they are retrieved, suggesting cell-autonomous processes, while MT-ARM requires *dnc* activity in other parts of the brain, involving circuit-scale mechanisms.

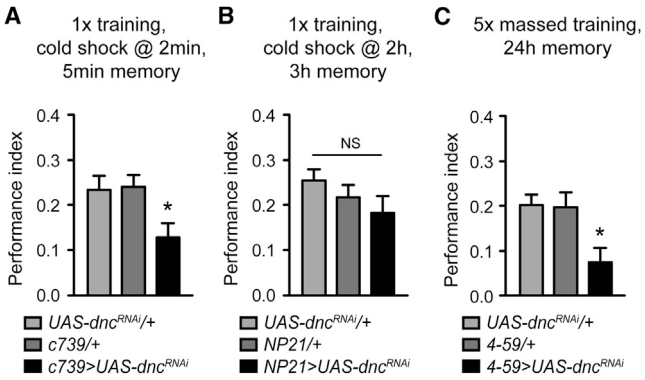

Figure 6. Localization of *dnc* Requirement for the Sequential ARM Phases

(A) The expression of an RNAi against *dnc* in α/β KCs with the c739 driver impaired ST-ARM ($F_{(2,26)}$ = 4.54, p = 0.02, n = 9).

(B) The expression of the same RNAi in γ KCs with the NP21 driver failed to impair MT-ARM ($F_{(2,39)}$ = 1.31, p = 0.28, n = 11–17).

(C) The expression of the RNAi against *dnc* in α′/β′ KCs with the 4-59 driver impaired LT-ARM ($F_{(2,40)}$ = 5.91, p = 0.0058, n = 12–15).

Data are mean ± SEM. *p < 0.05; NS, not significant. See Experimental Procedures for further details on statistical analyses.

DISCUSSION

In *Drosophila*, memory phases have historically been characterized behaviorally through the identification of specific mutants or through experimental features (e.g., resistance to cold shock or sensitivity to protein synthesis inhibitors). Based on these approaches, four aversive memory phases were previously documented: STM, MTM, ARM, and LTM. This study aimed to bridge the network and behavioral levels through a comprehensive dissection of the circuits involved in aversive memory retrieval at different time points after training, for both labile and anesthesia-resistant forms of memory. The role of MB neurons in all of these memories has long been established, but the identification of MB efferent neurons mediating memory retrieval is much more fragmented. In particular, STM is thought to be encoded in γ KCs, although the only output neurons that have been described so far project from the MB vertical lobes (Séjourné et al., 2011; Pai et al., 2013). Importantly, we have established the characterization of M6 neurons and, to a lesser extent, the M4 neurons as an additional type of MB output neuron for memory retrieval, particularly in STM retrieval. The other main conclusion from our work is that ARM, previously considered as a singular memory phase, can be split into three distinct temporal phases: ST-ARM, MT-ARM, and LT-ARM, which rely on distinct sets of KCs and MB output neurons. Interestingly, a recent independent study also identified M4 and M6 neurons as necessary for the retrieval of immediate memory, both aversive and appetitive (Owald et al., 2015). Here, we investigated in detail the recruitment of the different retrieval circuits by the distinct spatiotemporal components of aversive memory. Altogether, our study strikingly confirms that the behavioral distinction of memory phases is clearly reflected at the level of neural networks, since a specific circuit can be assigned to each form of memory at a given time point (Figure 7).

A single aversive training cycle generates pairs of memories that are independently encoded and retrieved in time and space. Immediately after training, STM is retrieved from γ KCs via the M4/M6 neurons. Simultaneously, ST-ARM is retrieved from α/β KCs by the V2α neurons (Figure 7). It is currently technically impossible to image odor responses in these cell types within the timescale dictated by the short persistence of STM and ST-ARM. Indeed, this would require development of a setup to train flies directly under the microscope, but such experiments could be revealing. Blocking M4 neurons (projecting from the β′ lobes) and M6 neurons (projecting from the γ and β′ lobes) impaired STM retrieval; however, blocking either M4 or M6 neurons alone surprisingly failed to block STM retrieval. This indicates that these two neurons can serve redundant functions in STM retrieval. Consistent with this hypothesis, another study also reported that simultaneous blocking of M4 and M6 neurons much strongly impaired immediate aversive or appetitive memory than blocking of M6 neurons alone (Owald et al., 2015). It is possible that the α′/β′ KC-M4 circuit is recruited as an alternative in case the default γ KC-M6 circuit is disrupted or damaged. Nonetheless, this redundancy does not exist at the KC level, since blocking γ KCs alone was sufficient to alter STM. Thus, the alternative circuit should also involve communication between γ and α′/β′ KCs, through a mechanism that remains to be identified. Such a functional redundancy could guarantee the robustness of STM retrieval despite a minimum number of M6 neurons.

During the 3-hr range after training, MTM is retrieved from α/β KCs by V2α neurons, and MT-ARM is retrieved from γ KCs via the M6 neurons (Figure 7). The respective assignments of labile and anesthesia-resistant memory components are thus inverted, as compared to immediate memory. Whether distinct forms of memory involve the same sets of neurons, and therefore act on the same synapses, has long been a subject of interest (Schwaerzel et al., 2003; Perisse et al., 2013). Although our understanding of the physiological processes underlying labile and anesthesia-resistant forms of memory is still limited, the identification of the separate output circuits for distinct forms of simultaneous memories reported herein provides an insight into their distinguishing features. Calcium imaging of odor responses 3 hr after training has been performed in V2 neurons (Séjourné et al., 2011) (for the retrieval of MTM), as well as in M6 neurons (for the retrieval of MT-ARM, present work). Interestingly, training has dramatically opposite effects on the olfactory responses of these two cell types. V2 neurons respond to odors with a strong phasic increase in activity, and training decreases the response to the CS^+ odorant as compared to CS^-. On the contrary, M6 neurons display a moderate but prolonged increase in the relative response to CS^+. This major mechanistic difference could explain why these distinct forms of memory cannot involve the same synapses, and hence the same circuits of KC-output neurons. Further studies are required to confirm whether this spatial segregation results from mutually antagonist or incompatible mechanisms.

In the 24-hr range, the LT-ARM formed after massed training is retrieved from α′/β′ KCs by M6 neurons. In a previous study, we reported a memory retrieval defect 24 hr after massed training by blocking V2 neurons with MZ160 or NP2492 driver (Séjourné

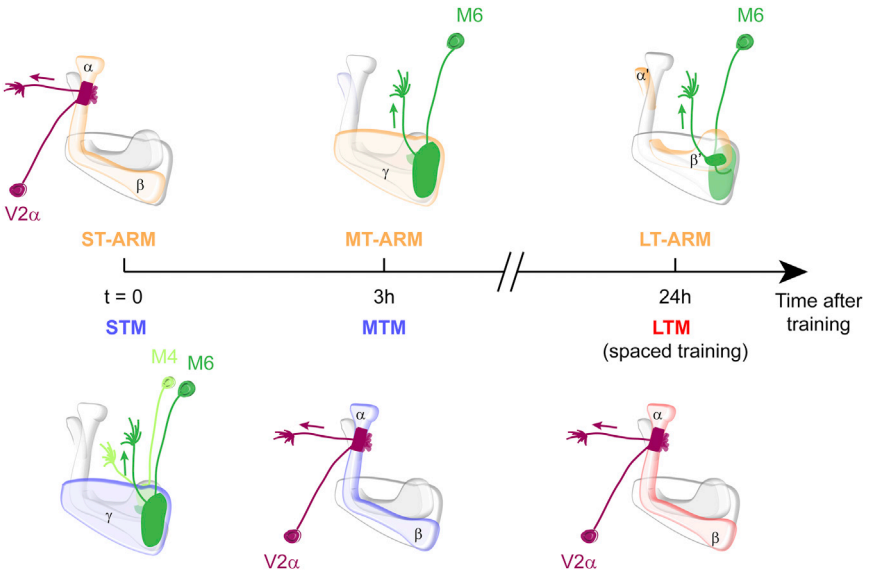

Figure 7. Spatiotemporal Distribution of Six Aversive Memory Phases in *Drosophila*

Summary of the memory encoding and retrieval circuits. The timeline indicates the time after training. STM, short-term memory; ST-ARM, short-term anesthesia-resistant memory; MTM, middle-term memory; MT-ARM, middle-term anesthesia-resistant memory; LTM, long-term memory; LT-ARM, long-term anesthesia-resistant memory. ARM circuits are shown above the time axis. The KC subset involved at a given time point is highlighted in orange. Circuits of STM and MTM are shown below the time axis. The KC subset involved at a given time point is highlighted in blue. When involved, V2 neurons are represented in purple and M4/M6 neurons in green. Left: STM and ST-ARM are both present immediately after training. STM retrieval involves the γ KC-M4/6 glutamatergic neuron circuit and ST-ARM retrieval involves the α/β KC-V2α cholinergic neuron circuit. Middle: MTM and MT-ARM are simultaneously expressed 3 hr after training. The circuit attribution is reversed compared to immediate memory: MTM retrieval involves the α/β KC-V2α neuron circuit and MT-ARM retrieval involves the γ KC-M6 neuron circuit. Right: 24 hr after training, flies can display either LT-ARM or LTM depending on the conditioning protocol. Hence, contrary to other time points these two memories are not simultaneously present. After massed training, LT-ARM retrieval involves the α′/β′ KC-M6 neuron circuit. After spaced training, LTM involves the α/β KC-V2α neurons circuit.

et al., 2011). In contradiction with this previous report, we did not measure a defect with the MZ160 driver 24 hr after massed training (Figure S5O). The fact that no defect was observed with the 71D08 driver (Figure 5E) strongly suggests that an unfortunate error occurred in the crosses used in our former massed training experiment with the MZ160 driver (for example, that the NP2492 driver was used instead of the MZ160 one) (Figure 4 in Séjourné et al., 2011). In the present study, we additionally showed that the LT-ARM defect observed with the NP2492 driver is due to non-cholinergic signaling (Figures S5P–S5R) and hence attributable to neurons other than V2. Collectively, our results indicate that LT-ARM is retrieved by M6 neurons.

LTM, which forms after spaced training, is encoded in α/β KCs according to several convergent reports (Huang et al., 2013; Isabel et al., 2004; Yu et al., 2006) and is retrieved via the V2 neurons (Séjourné et al., 2011; Aso et al., 2014b) (Figure 7). Previously, we reported that LTM formation is gated during the inter-trial intervals of a spaced training by the activity of at most three pairs of PPL1 dopaminergic neurons projecting on the MB lobes (Plaçais et al., 2012). As the activity of the same neurons has an adverse effect on ARM (Plaçais et al., 2012), we have proposed a model of LTM formation in which ARM and LTM are the products of antagonist consolidation pathways (Isabel et al., 2004). The ARM pathway is fully inhibited during spaced training to allow for LTM formation. Now that we have established that ARM is divided into three distinct phases, it can be asked which ARM phase inhibits LTM formation. Two separate lines of arguments advocate ST-ARM for this role. First, ST-ARM occurs on a timescale that is highly compatible with the gating that occurs over the 1.5-hr duration of the spaced training. Second, the location of LTM in the α/β KCs is firmly documented (Huang et al., 2012; Pascual and Préat, 2001; Yu et al., 2006), and ST-ARM also relies on the α/β KCs. It is thus possible that cellular mechanisms underlying ST-ARM antagonize LTM formation through intra-α/β KCs processes. Overall, our study revealing composite memory circuits sheds light on how to address the questions of memory phase interaction and systems consolidation (Dubnau and Chiang, 2013).

EXPERIMENTAL PROCEDURES

Fly Strains

All transgenic lines were outcrossed for five generations to a w^{1118} strain in a wild-type *Canton-Special* (*CS*) background. For behavioral experiments, except those shown on Figure 6, flies were raised on standard medium containing yeast cornmeal and agar at 18°C and 60% humidity under a 12-hr:12-hr light-dark cycle. For behavioral experiments using the *dnc* RNAi, flies were raised at 25°C and adult flies were kept at 30.5°C for 3 days before the experiment (Scheunemann et al., 2012). For imaging and immunohistochemistry experiments, flies were raised at 25°C. See the Supplemental Experimental Procedures for more details.

Behavior Experiments

For all behavior experiments, 0- to 2-day-old flies were transferred to fresh food vials the day before conditioning. Conditioning and tests of memory performance and of olfactory acuity were performed essentially as described previously (Séjourné et al., 2011) (see the Supplemental Experimental Procedures for more details). The two odorants used in these experiments were 3-octanol and 4-methylcyclohexanol. Cold anesthesia was achieved by a 2-min cold shock performed either 2 min after training (for ST-ARM) or 2 hr after training (for MT-ARM). An exception was made for experiments shown in Figures S1T and S1U for which cold shock was performed 1 hr after training and the memory test performed 2 hr after training to match the conditions used in our previous study (Isabel et al., 2004). Under these conditions, labile memory was now located in α/β KCs and ARM in γ KCs, which corresponds to the characteristics of MTM and MT-ARM (Figures S1T and S1U). On the contrary, in our previous study (Isabel et al., 2004), labile memory and ARM measured 2 hr after training with a cold shock performed 1 hr after training were located respectively in γ and α/β KCs and thus most likely corresponded to STM and ST-ARM. This apparent contradiction suggests that over the past 11 years

some parameter has evolved in our laboratory, causing a slight shift in the kinetics of the transition from STM and ST-ARM patterns to MTM and MT-ARM ones. This might be due, for instance, to a modification in our fly food recipe, which has been improved with a change in yeast. We now use the Springaline BA10/0 reference from Lesaffre (France).

Memory scores are displayed as mean ± SEM. A single value of the performance index is the average of two scores obtained from two groups of genetically identical flies conditioned in two reciprocal experiments, using either odorant as CS^+. The indicated "*n*" is the number of independent values of the performance index for each genotype. Unless stated otherwise (Figure 1A; Figure S5A), statistical analyses were performed by one-way ANOVA followed by Newman-Keuls pairwise comparisons. The asterisks displayed on the bar plots indicate the least significant pairwise post hoc comparisons between the flies of the genotype of interest and the flies of other genotypes. *$p < 0.05$; **$p < 0.01$; ***$p < 0.0001$; NS, not significant.

Immunohistochemistry

Flies from GAL4 lines were crossed to *UAS-mCD8::GFP* flies. Brains of female F1 progenies (3–4 days after eclosion at 25°C) were prepared for anti-GFP immunohistochemistry and anti-nc82 for counterstaining. Images were acquired with a Nikon A1R confocal microscope and imported into ImageJ for analyses. See the Supplemental Experimental Procedures for more details.

In Vivo Calcium Imaging

0- to 2-day-old flies were transferred to a fresh food vial the day before the experiment and then trained with one cycle of aversive conditioning or an unpaired aversive protocol and maintained on food afterward until preparation for in vivo imaging. Flies received the same number of electric shocks during an unpaired protocol as during a standard associative conditioning cycle, and then 2 min later they were delivered the first odorant (the "CS^+") for 1 min; 45 s later, the second odorant (the "CS^-") was presented for 1 min. Data were collected in equal proportion from flies presented with either octanol or methylcyclohexanol as the CS^+ (or "CS^+" for unpaired-trained flies).

For in vivo imaging, one female fly was prepared essentially as described previously (Séjourné et al., 2011), with the exception that ribose replaced sucrose at the same concentration in the solution bathing the brain. The fly was then placed under the objective lens (25×, 0.95 NA) of a confocal microscope under a constant airflow of 1.5 l × min^{-1}. Images were acquired at a rate of one 512 × 150 image every 412 ms. The emitted light was collected from transverse sections of the brain showing dorsal presynaptic projections of M6 neurons in the SMP region. In general, both hemispheres could be recorded simultaneously. See the Supplemental Experimental Proceduresfor more details.

SUPPLEMENTAL INFORMATION

Supplemental Information includes Supplemental Experimental Procedures and five figures and can be found with this article online at http://dx.doi.org/10.1016/j.celrep.2015.04.044.

AUTHOR CONTRIBUTIONS

E.B., S.T., L.S., and P.-Y.P. performed the experiments. P.-Y.P. and E.B. prepared the figures. P.-Y.P. and T.P. wrote the manuscript and supervised the work. All authors commented on the manuscript.

ACKNOWLEDGMENTS

We thank the Janelia Farm FlyLight Project Team and the Dickson group for making available the GMR and VT GAL4 collections, respectively. We thank Aurélie Lampin-Saint-Amaux for assistance in experimental work and Valérie Goguel for critical comments on the manuscript. E.B. was supported by a doctoral fellowship from the French Ministry of Research. E.B. and S.T. were funded by the Fondation pour la Recherche Médicale. L.S. was funded by the Ecole des Neurosciences de Paris Ile-de-France and by the Deutsche Forschungsgemeinschaft (DFG GZ: SCHE 1884/1-1). This work was supported by the Agence Nationale pour la Recherche (to T.P.).

Received: November 14, 2014
Revised: February 27, 2015
Accepted: April 21, 2015
Published: May 14, 2015

REFERENCES

Aso, Y., Grübel, K., Busch, S., Friedrich, A.B., Siwanowicz, I., and Tanimoto, H. (2009). The mushroom body of adult Drosophila characterized by GAL4 drivers. J. Neurogenet. *23*, 156–172.

Aso, Y., Hattori, D., Yu, Y., Johnston, R.M., Iyer, N.A., Ngo, T.T., Dionne, H., Abbott, L.F., Axel, R., Tanimoto, H., and Rubin, G.M. (2014a). The neuronal architecture of the mushroom body provides a logic for associative learning. eLife *3*, e04577.

Aso, Y., Sitaraman, D., Ichinose, T., Kaun, K.R., Vogt, K., Belliart-Guérin, G., Plaçais, P.Y., Robie, A.A., Yamagata, N., Schnaitmann, C., et al. (2014b). Mushroom body output neurons encode valence and guide memory-based action selection in Drosophila. eLife *3*, e04580.

Blum, A.L., Li, W., Cressy, M., and Dubnau, J. (2009). Short- and long-term memory in Drosophila require cAMP signaling in distinct neuron types. Curr. Biol. *19*, 1341–1350.

Cervantes-Sandoval, I., Martin-Peña, A., Berry, J.A., and Davis, R.L. (2013). System-like consolidation of olfactory memories in Drosophila. J. Neurosci. *33*, 9846–9854.

Colomb, J., Kaiser, L., Chabaud, M.-A., and Preat, T. (2009). Parametric and genetic analysis of Drosophila appetitive long-term memory and sugar motivation. Genes Brain Behav. *8*, 407–415.

Comas, D., Petit, F., and Preat, T. (2004). Drosophila long-term memory formation involves regulation of cathepsin activity. Nature *430*, 460–463.

Crittenden, J.R., Skoulakis, E.M., Han, K.A., Kalderon, D., and Davis, R.L. (1998). Tripartite mushroom body architecture revealed by antigenic markers. Learn. Mem. *5*, 38–51.

de Belle, J.S., and Heisenberg, M. (1994). Associative odor learning in Drosophila abolished by chemical ablation of mushroom bodies. Science *263*, 692–695.

Didelot, G., Molinari, F., Tchénio, P., Comas, D., Milhiet, E., Munnich, A., Colleaux, L., and Preat, T. (2006). Tequila, a neurotrypsin ortholog, regulates long-term memory formation in Drosophila. Science *313*, 851–853.

Dubnau, J., and Chiang, A.-S. (2013). Systems memory consolidation in Drosophila. Curr. Opin. Neurobiol. *23*, 84–91.

Dubnau, J., Chiang, A.S., Grady, L., Barditch, J., Gossweiler, S., McNeil, J., Smith, P., Buldoc, F., Scott, R., Certa, U., et al. (2003). The staufen/pumilio pathway is involved in Drosophila long-term memory. Curr. Biol. *13*, 286–296.

Dudai, Y., Jan, Y.N., Byers, D., Quinn, W.G., and Benzer, S. (1976). dunce, a mutant of Drosophila deficient in learning. Proc. Natl. Acad. Sci. USA *73*, 1684–1688.

Gerber, B., Tanimoto, H., and Heisenberg, M. (2004). An engram found? Evaluating the evidence from fruit flies. Curr. Opin. Neurobiol. *14*, 737–744.

Heisenberg, M. (2003). Mushroom body memoir: from maps to models. Nat. Rev. Neurosci. *4*, 266–275.

Huang, C., Zheng, X., Zhao, H., Li, M., Wang, P., Xie, Z., Wang, L., and Zhong, Y. (2012). A permissive role of mushroom body α/β core neurons in long-term memory consolidation in Drosophila. Curr. Biol. *22*, 1981–1989.

Huang, C., Wang, P., Xie, Z., Wang, L., and Zhong, Y. (2013). The differential requirement of mushroom body α/β subdivisions in long-term memory retrieval in Drosophila. Protein Cell *4*, 512–519.

Isabel, G., Pascual, A., and Preat, T. (2004). Exclusive consolidated memory phases in Drosophila. Science *304*, 1024–1027.

Jenett, A., Rubin, G.M., Ngo, T.T., Shepherd, D., Murphy, C., Dionne, H., Pfeiffer, B.D., Cavallaro, A., Hall, D., Jeter, J., et al. (2012). A GAL4-driver line resource for Drosophila neurobiology. Cell Rep. *2*, 991–1001.

Kaun, K.R., Azanchi, R., Maung, Z., Hirsh, J., and Heberlein, U. (2011). A Drosophila model for alcohol reward. Nat. Neurosci. *14*, 612–619.

Kitamoto, T. (2001). Conditional modification of behavior in Drosophila by targeted expression of a temperature-sensitive shibire allele in defined neurons. J. Neurobiol. *47*, 81–92.

Knapek, S., Sigrist, S., and Tanimoto, H. (2011). Bruchpilot, a synaptic active zone protein for anesthesia-resistant memory. J. Neurosci. *31*, 3453–3458.

Krashes, M.J., and Waddell, S. (2008). Rapid consolidation to a radish and protein synthesis-dependent long-term memory after single-session appetitive olfactory conditioning in Drosophila. J. Neurosci. *28*, 3103–3113.

Krashes, M.J., Keene, A.C., Leung, B., Armstrong, J.D., and Waddell, S. (2007). Sequential use of mushroom body neuron subsets during Drosophila odor memory processing. Neuron *53*, 103–115.

Lee, P.-T., Lin, H.-W., Chang, Y.-H., Fu, T.-F., Dubnau, J., Hirsh, J., Lee, T., and Chiang, A.-S. (2011). Serotonin-mushroom body circuit modulating the formation of anesthesia-resistant memory in Drosophila. Proc. Natl. Acad. Sci. USA *108*, 13794–13799.

Liu, G., Seiler, H., Wen, A., Zars, T., Ito, K., Wolf, R., Heisenberg, M., and Liu, L. (2006). Distinct memory traces for two visual features in the Drosophila brain. Nature *439*, 551–556.

McBride, S.M., Giuliani, G., Choi, C., Krause, P., Correale, D., Watson, K., Baker, G., and Siwicki, K.K. (1999). Mushroom body ablation impairs short-term memory and long-term memory of courtship conditioning in Drosophila melanogaster. Neuron *24*, 967–977.

McGuire, S.E., Le, P.T., and Davis, R.L. (2001). The role of Drosophila mushroom body signaling in olfactory memory. Science *293*, 1330–1333.

Owald, D., Felsenberg, J., Talbot, C.B., Das, G., Perisse, E., Huetteroth, W., and Waddell, S. (2015). Activity of defined mushroom body output neurons underlies learned olfactory behavior in Drosophila. Neuron *86*, 417–427.

Pai, T.-P., Chen, C.-C., Lin, H.-H., Chin, A.-L., Lai, J.S.-Y., Lee, P.-T., Tully, T., and Chiang, A.-S. (2013). Drosophila ORB protein in two mushroom body output neurons is necessary for long-term memory formation. Proc. Natl. Acad. Sci. USA *110*, 7898–7903.

Pascual, A., and Préat, T. (2001). Localization of long-term memory within the Drosophila mushroom body. Science *294*, 1115–1117.

Perisse, E., Yin, Y., Lin, A.C., Lin, S., Huetteroth, W., and Waddell, S. (2013). Different kenyon cell populations drive learned approach and avoidance in Drosophila. Neuron *79*, 945–956.

Plaçais, P.-Y., Trannoy, S., Isabel, G., Aso, Y., Siwanowicz, I., Belliart-Guérin, G., Vernier, P., Birman, S., Tanimoto, H., and Preat, T. (2012). Slow oscillations in two pairs of dopaminergic neurons gate long-term memory formation in Drosophila. Nat. Neurosci. *15*, 592–599.

Qin, H., Cressy, M., Li, W., Coravos, J.S., Izzi, S.A., and Dubnau, J. (2012). Gamma neurons mediate dopaminergic input during aversive olfactory memory formation in Drosophila. Curr. Biol. *22*, 608–614.

Quinn, W.G., and Dudai, Y. (1976). Memory phases in Drosophila. Nature *262*, 576–577.

Quinn, W.G., Sziber, P.P., and Booker, R. (1979). The Drosophila memory mutant amnesiac. Nature *277*, 212–214.

Schacter, D.L., and Tulving, E. (1994). Memory Systems 1994 (MIT Press).

Scheunemann, L., Jost, E., Richlitzki, A., Day, J.P., Sebastian, S., Thum, A.S., Efetova, M., Davies, S.-A., and Schwärzel, M. (2012). Consolidated and labile odor memory are separately encoded within the Drosophila brain. J. Neurosci. *32*, 17163–17171.

Schwaerzel, M., Monastirioti, M., Scholz, H., Friggi-Grelin, F., Birman, S., and Heisenberg, M. (2003). Dopamine and octopamine differentiate between aversive and appetitive olfactory memories in Drosophila. J. Neurosci. *23*, 10495–10502.

Séjourné, J., Plaçais, P.Y., Aso, Y., Siwanowicz, I., Trannoy, S., Thoma, V., Tedjakumala, S.R., Rubin, G.M., Tchénio, P., Ito, K., et al. (2011). Mushroom body efferent neurons responsible for aversive olfactory memory retrieval in Drosophila. Nat. Neurosci. *14*, 903–910.

Stough, S., Shobe, J.L., and Carew, T.J. (2006). Intermediate-term processes in memory formation. Curr. Opin. Neurobiol. *16*, 672–678.

Tanaka, N.K., Tanimoto, H., and Ito, K. (2008). Neuronal assemblies of the Drosophila mushroom body. J. Comp. Neurol. *508*, 711–755.

Tempel, B.L., Bonini, N., Dawson, D.R., and Quinn, W.G. (1983). Reward learning in normal and mutant Drosophila. Proc. Natl. Acad. Sci. USA *80*, 1482–1486.

Trannoy, S., Redt-Clouet, C., Dura, J.-M., and Preat, T. (2011). Parallel processing of appetitive short- and long-term memories in Drosophila. Curr. Biol. *21*, 1647–1653.

Tully, T., Preat, T., Boynton, S.C., and Del Vecchio, M. (1994). Genetic dissection of consolidated memory in Drosophila. Cell *79*, 35–47.

Wang, Y., Mamiya, A., Chiang, A.-S., and Zhong, Y. (2008). Imaging of an early memory trace in the Drosophila mushroom body. J. Neurosci. *28*, 4368–4376.

Xie, Z., Huang, C., Ci, B., Wang, L., and Zhong, Y. (2013). Requirement of the combination of mushroom body γ lobe and α/β lobes for the retrieval of both aversive and appetitive early memories in Drosophila. Learn. Mem. *20*, 474–481.

Yin, J.C., Wallach, J.S., Del Vecchio, M., Wilder, E.L., Zhou, H., Quinn, W.G., and Tully, T. (1994). Induction of a dominant negative CREB transgene specifically blocks long-term memory in Drosophila. Cell *79*, 49–58.

Yu, D., Akalal, D.-B.G., and Davis, R.L. (2006). Drosophila α/β mushroom body neurons form a branch-specific, long-term cellular memory trace after spaced olfactory conditioning. Neuron *52*, 845–855.